On the Outage Performance of Ambient Backscatter Communications

Yinghui Ye, Liqin Shi, Xiaoli Chu, *Senior Member, IEEE*, and Guangyue Lu

Abstract—Ambient backscatter communications (AmBack-Coms) have been recognized as a spectrum- and energy-efficient technology for Internet of Things, as it allows passive backscatter devices (BDs) to modulate their information into the legacy signals, e.g., cellular signals, and reflect them to their associated receivers while harvesting energy from the legacy signals to power their circuit operation. However, the co-channel interference between the backscatter link and the legacy link and the non-linear behavior of energy harvesters at the BDs have largely been ignored in the performance analysis of AmBackComs. Taking these two aspects, this paper provides a comprehensive outage performance analysis for an AmBackCom system with multiple backscatter links, where one of the backscatter links is opportunistically selected to leverage the legacy signals transmitted in a given resource block. For any selected backscatter link, we propose an adaptive reflection coefficient (RC), which is adapted to the non-linear energy harvesting (EH) model and the location of the selected backscatter link, to minimize the outage probability of the backscatter link. In order to study the impact of co-channel interference on both backscatter and legacy links, for a selected backscatter link, we derive the outage probabilities for the legacy link and the backscatter link. Furthermore, we study the best and worst outage performances for the backscatter system where the selected backscatter link maximizes or minimizes the signal-to-interference-plus noise ratio (SINR) at the backscatter receiver. We also study the best and worst outage performances for the legacy link where the selected backscatter link results in the lowest and highest co-channel interference to the legacy receiver, respectively. Computer simulations validate our analytical results, and reveal the impacts of the co-channel interference and the EH model on the AmBackCom performance. In particular, the co-channel interference leads to the outage saturation phenomenon in AmBackComs, and the conventional linear EH model results in an over-estimated outage performance for the backscatter link.

Index Terms—Ambient backscatter communication, non-linear energy harvesting, co-channel interference, outage probability.

I. INTRODUCTION

Yinghui Ye and Liqin Shi are with the Shaanxi Key Laboratory of Information Communication Network and Security, Xi'an University of Posts & Telecommunications, China, and are also with the School of Telecommunication Engineering, Xidian University, China. (e-mail: connectyyh@126.com, liqinshi@hotmail.com)

Xiaoli Chu is with the Department of Electronic and Electrical Engineering, The University of Sheffield, U.K. (e-mail: x.chu@sheffield.ac.uk)

Guangyue Lu is with the Shaanxi Key Laboratory of Information Communication Network and Security, Xi'an University of Posts and Telecommunications (e-mail: tonylugy@163.com)

IN the era of Internet of Things (IoT), a great number of devices will be deployed to monitor, sense, and generate enormous data, in order to support different applications, e.g., smart city, and intelligent agriculture. It is predicted by Ericsson that about 22.3 billion IoT devices will be deployed worldwide by 2024 [1]. The development of massive IoT devices is facing different challenges caused by the limited battery capacity of IoT deveices and the limited spectrum resource. In this context, ambient backscatter communication (AmBackCom) has been considered as a potential solution to address these two challenges [2], [3]. In AmBackComs, the backscatter device (BD) modulates its message on the received legacy signals, e.g., cellular or WiFi signals, and reflects the modulated signals to its associated receiver, while harvesting energy from the legacy signals for covering the circuit energy consumption [4], [5]. This is different from the simultaneous wireless information and power transfer (SWIPT), where the transmitter generates radio frequency (RF) signals itself for conveying energy and information to the receiver simultaneously. Thus, the BD does not need active components, e.g., oscillators, analog-to-digital/digital-to-analog converters, resulting in a much less energy consumption as compared with a SWIPT transmitter [2], [6]. Meanwhile, the backscatter link shares the same spectrum resource with the legacy link, i.e., no extra spectrum resource is required for AmBackComs.

Due to the spectrum sharing between the legacy link and the backscatter link, there will be co-channel interference between them. Symbol detectors have been proposed for THE backscatter receiver (BR) to suppress the co-channel interference caused by the legacy transmitter (LT). In [7], for the differential on-off modulation, a maximum a posteriori (MAP) based detector was proposed by exploiting the difference between two consecutive signal powers. In [8], a semi-coherent detection was developed based on the likelihood ratio test. Exploiting the advantages of multiple antennas, the authors of [9] proposed a maximum-eigenvalue detector and demonstrated its superior symbol detection performance by comparing with the energy-based detector. In [10], the ambient waveform and the symbol detector were jointly designed for orthogonal frequency division multiplexing (OFDM) systems. The above works mainly focus on the detectors design and characterizing the achievable bit error rate for backscatter links, but have not considered the outage performance.

In addition to [8]–[10], there are a considerable number of studies on the design of resource allocation schemes for AmBackComs. In [11]–[18], the authors proposed harvest-then-transmit (HTT) enabled AmBackComs, and designed resource allocation schemes to satisfy various optimization goals. In

Table I Definitions of Notations

Notation	Meaning
α	Path loss exponent
$\mathbb{P}(\cdot)$	Probability operator
$\mathbb{E}[\cdot]$	Expectation operator
P_t	Transmit power of the LT
Λ_{1k}	Frequency dependent constant
β_k	Reflection coefficient of the k-th BD
$P_{c,k}$	Circuit power consumption at the k-th BD
T	A whole time slot of the legacy transmission
$\mathcal{CN}(a,b)$	Gaussian distribution with mean a and variance b
γ_{th}^b and γ_{th}	SINR threshold for the k-th backscatter link and the legacy link
$\mathcal{P}_{\text{out},k}^b$ and $\mathcal{P}_{\text{out},k}^l$	Outage probability for the k-th backscatter link and the legacy link
h_p and d_p	Channel coefficient and distance of the legacy link
g_k^p and d_k^p	Channel coefficient and distance of the LT-to-the k-th BR link ($k \in \{1,\cdots,K\}$)
h_{1k} and d_{1k}	Channel coefficient and distance of the LT-to-the k-th BD link ($k \in \{1,\cdots,K\}$)
h_{2k} and d_{2k}	Channel coefficient and distance of the k-th backscatter link ($k \in \{1,\cdots,K\}$)
g_k^s and d_k^s	Channel coefficient and distance of the k-th BD-to-LR link ($k \in \{1,\cdots,K\}$)

these works, they mainly focused on balancing the time allocation between the backscatter mode and the HTT mode in order to maximize the achievable throughput of backscatter links based on a fixed transmission rate of backscatter links, i.e., the reflection coefficient (RC) of BDs and the transmit power of the LT are fixed. By assuming that both the RC of BDs and the transmit power of the LT can be adjusted, the resource allocation scheme was designed in the coexistence of cognitive networks and AmbackComs [19], where the sum throughput of the backscatter link is maximized. AmbackCom was combined with full-duplex transmissions in [20], where a full-duplex access point simultaneously transmits signals to its legacy receiver (LR) and receives the backscattered signals from BDs, and the fairness among the backscatter links in terms of the achievable throughput is guaranteed.

The performance analysis in terms of ergodic capacity and outage probability has also been investigated in AmBackComs. In [21], the ergodic capacity of the backscatter link with a two-state modulation was derived in the case of real or complex RF signals. In [22], the authors analyzed the ergodic capacity in the coexistence of AmBackComs and legacy systems that employ an OFDM scheme. In [23], the authors analyzed the ergodic rate for legacy and backscatter links, where the BD and the BR are co-located. In [24], the author proposed an opportunistic AmBackCom-assisted decode-and-forward relay network, and derived a closed-form expression of the achievable ergodic capacity. The outage probability of a backscatter link was analyzed in [25], where multiple antennas and maximum ratio combing were employed at the BR, but the outage performance of the legacy link was not studied. Using tools from stochastic geometry, the outage probabilities and achievable rates for the legacy and backscatter links were investigated [26]. The authors in [27] derived the outage probability of the backscatter link for a two-state modulation at the BD. The authors of [28] considered the backscatter links as the secondary users in a cognitive relay network, and derived the outage probabilities of both the primary and backscatter links. In [29], the authors proposed a novel hybrid device-to-device (D2D) transmitter that alternately operates in the backscatter mode and the HTT mode, and analyzed the outage probability and the average outage capacity. However, there are limitations in the above existing works, which are listed below.

- The studies in [22]–[25], [28] assumed that the BR was able to successfully decode the legacy signals and perform a perfect successive interference cancellation (SIC) to remove the interference brought by the LT. The authors of [26], [29] ignored the interference from the LT to the backscatter links. In addition, the outage performance of legacy links has largely been ignored [25], [27], [29]. Therefore, there is a lack of a comprehensive performance analysis for AmBackComs.

- In AmBackComs, an energy outage event at the backscatter link occurs when the harvested energy at the BD cannot meet the circuit consumption. Hence, the performance analysis of AmBackComs requires an accurate model for the harvested energy. In [21] and [27], the energy outage event was not considered. The studies [11]–[17], [19], [20], [22]–[26], [28], [29] assume a linear energy harvesting (EH) model at the BD, which fails to characterize the inherent non-linearity of a practical energy harvester [30]–[32]. The use of an inaccurate EH model will affect the accuracy of signal-to-interference-plus-noise ratios (SINRs) for both legacy and backscatter links. Thus, it is desirable to consider a non-linear EH model in the performance analysis for AmBackComs.

In this paper, we take the above observations into account and analyze the outage probability of an AmBackCom network. In particular, we consider an AmBackCom network with multiple backscatter links, where only one backscatter link is opportunistically selected to backscatter the legacy signal transmitted in any given resource block, thus avoiding severe co-channel interference among backscatter links.

Our main contributions are summarized as follows.

- Considering a practical non-linear EH model, we propose an adaptive RC scheme to minimize the outage probability for any selected backscatter link and obtain a closed-form expression for the optimal RC, which provides a guideline for BDs to set the value of RC in a practical backscatter communication system. With the optimal RC and a selected backscatter link, the outage probabilities for the backscatter link and the legacy link are derived. The outage-probability lower bounds for both links are
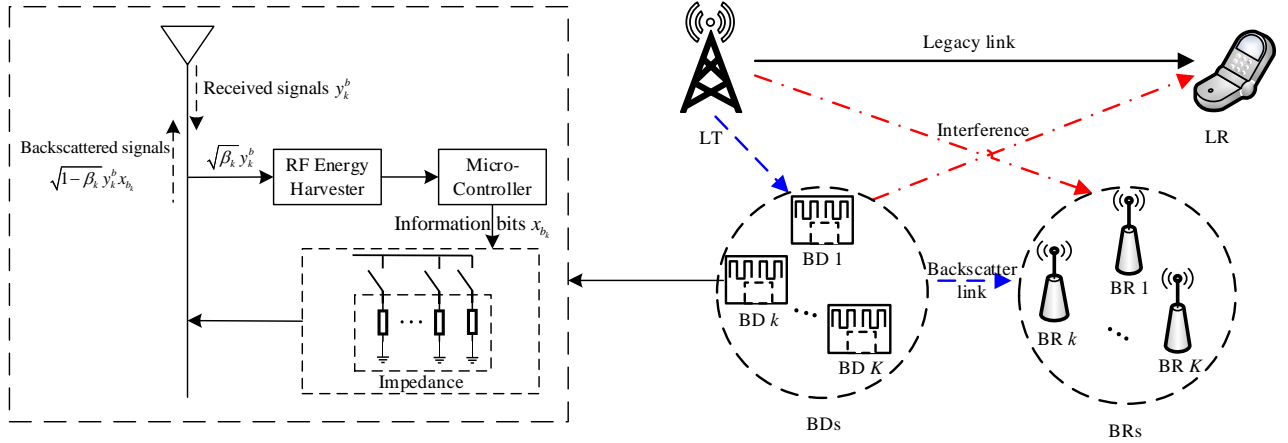
Fig. 1. System model: the left subgraph subplot shows the structure of the k-th BD, and the right subgraph subplot illustrates the AmBackCom network.

obtained as the transmit power of the LT approaches infinity.

- We evaluate the best and worst outage performances for the backscatter system and the legacy transmission, respectively. Specifically, the selected backscatter link with the maximum (or minimum) SINR at the BR leads to the best (or worst) outage performance for the backscatter system, while the selected backscatter resulting in the lowest (or highest) co-channel interference to the LR causes the best (or worst) outage performance for the legacy system.

- We examine the effects of co-channel interference and the EH model on the achievable outage probability of the considered AmBackCom network, and make the following new observations. Firstly, the co-channel interference between the backscatter link and the legacy link leads to an outage saturation phenomenon for both the backscatter and legacy links at a high transmit power of the LT. Secondly, the passive BD that causes the lowest co-channel interference to the LR can realize its own information transmission at the cost of a slightly degraded outage performance of the legacy link even for low or medium transmit power of the LT. Thirdly, the conventionally used linear EH model leads to a greatly over-estimated outage performance for the backscatter link and a slightly underrated outage performance for the legacy link.

The remainder of this paper is organized as follows. The system model is provided in Section II. Sections III and IV analyze the outage performance of the backscatter system and the legacy transmission, respectively. Numerical results are shown in Section V, followed by conclusions in Section VI. Besides, the main notations have been summarized in Table I, as shown at the top of the next page.

II. SYSTEM MODEL

In this work, we consider an AmBackCom network, which consists of one LT, one LR, and K BDs and their receivers, as shown in Fig. 1. In this network, the LT transmits its signal to the LR in a given resource block, forming a legacy radio link, while one of backscatter links is opportunistically selected to

modulate its information into the LT transmitted signal and backscatter the modulated signal to its own receiver. Assume that all channels are quasi-static and subject to path-loss and Rayleigh fading. Let h_p, g_k^p, h_{1k}, h_{2k} and g_k^s ($k \in \{1, \cdots, K\}$) denote the channel coefficients[1] of the legacy link, the LT-to-the k-th BR link, the LT-to-the k-th BD link, the k-th backscatter link, and the k-th BD-to-LR link, respectively. The corresponding distances are denoted by d_p, d_k^p, d_{1k}, d_{2k} and d_k^s, respectively.

For the legacy system, the LT transmits its information x_p with $\mathbb{E}[|x_p|^2] = 1$ to the LR. Meanwhile, the received signal at the k-th BD is given by

$$y_k^b = \sqrt{P_t \Lambda_{1k} d_{1k}^{-\alpha}} h_{1k} x_p + n_k^b, \tag{1}$$

where P_t is the transmit power of the LT; Λ_{1k} denotes the frequency dependent constant [34] for the LT-to-the k-th BD link; α is the path loss exponent and $n_k^b \sim \mathcal{CN}(0, \sigma^2)$ denotes the additive white Gaussian noise (AWGN) at the k-th BD.

Following [19], the received signals at the k-th BD is divided into two parts through a RC β_k: $\sqrt{\beta_k} y_k^b$ used for EH and the remaining one with $\sqrt{1 - \beta_k} y_k^b$ for backscattering. Here we consider a practical non-linear EH model proposed in [30] to characterize the harvested power. Then the total harvested energy at the k-th BD is given by

$$E_k = \frac{E_{\max,k} \left(1 - \exp\left(-s_{1k} P_{r,k} + s_{1k} s_{0k}\right)\right)}{1 + \exp\left(-s_{1k} P_{r,k} + s_{1k} s_{2k}\right)} T, \tag{2}$$

where $P_{r,k} = \beta_k P_t \Lambda_{1k} d_{1k}^{-\alpha} |h_{1k}|^2$ is the input RF power of the harvester at the k-th BD; $E_{\max,k}$ is the maximum harvestable power when the circuit is saturated; s_{0k} denotes the sensitivity threshold; s_{1k} and s_{2k} are fixed parameters determined by the

---

[1] The channel gains $|g_k^p|^2$ and $|h_{1k}|^2 |h_{2k}|^2$ can be estimated by using the channel estimation method proposed in [33]. Please note that $|h_{1k}|^2$ can be obtained after estimating $|h_{2k}|^2$, and $|h_{2k}|^2$ can be estimated using traditional channel estimation methods. Particularly, the k-th BR is a traditional node and can send a pilot signal to the k-th BD and then the k-th BD reflects the pilot signal to the k-th BR. By performing least-square estimation, the k-th BR can obtain the product of the forward channel gain and the backward channel gain. Due to the channel reciprocity, the forward channel gain equals the backward channel gain and hence $|h_{2k}|^2$ is obtained by taking the square root of the product.

resistance, capacitance, and diode turn-on voltage; T is the whole time slot for the legacy transmission.

Let $P_{c,k}$ denote the circuit power consumption at the k-th BD. When $E_k \geq P_{c,k}T$, the k-th BD has enough energy for the circuit operation. Otherwise, the k-th BD can not backscatter information to its receiver. For the above two cases, we can write the received SINR at the BR and LR as follows.

(i) If $E_k \geq P_{c,k}T$, the k-th BD can modulate its own information x_{b_k} with $\mathbb{E}[|x_{b_k}|^2] = 1$ on the received signal $\sqrt{1-\beta_k}y_k^b$, and reflect the modulated signals. Then the received signal from the k-th BD to its receiver is

$$y_k^r = \sqrt{\eta_k (1-\beta_k) P_t K_{1k} K_{2k}} h_{1k} h_{2k} x_p x_{b_k}$$
$$+ \sqrt{P_t K_k^p} g_k^p x_p + n_k^r, \quad (3)$$

where η_k denotes the backscatter efficiency [4] for the k-th BD, $K_{1k} = \Lambda_{1k} d_{1k}^{-\alpha}$, $K_{2k} = \Lambda_{2k} d_{2k}^{-\alpha}$, $K_k^p = \Lambda_k^p (d_k^p)^{-\alpha}$ with the frequency dependent constant for the LT-to-the k-th BR link Λ_k^p, and $n_k^r \sim \mathcal{CN}(0,\sigma^2)$ is the AWGN at the k-th BR. Accordingly, the SINR for decoding x_{b_k} at the BR can be written as

$$\gamma_k^b = \frac{\eta_k (1-\beta_k) P_t K_{1k} K_{2k} |h_{1k}|^2 |h_{2k}|^2}{P_t K_k^p |g_k^p|^2 + \sigma^2}. \quad (4)$$

Since the backscattered signals cause interference to the LR, the received signal at the LR is given by

$$y_k^{(1)} = \sqrt{\eta_k (1-\beta_k) P_t K_{1k} K_k^s} h_{1k} g_k^s x_p x_{b_k}$$
$$+ \sqrt{P_t K_p} h_p x_p + n_p \quad (5)$$

where $K_p = \Lambda_p d_p^{-\alpha}$, $K_k^s = \Lambda_k^s (d_k^s)^{-\alpha}$, Λ_p and Λ_k^s are the frequency dependent constants for the legacy link and the k-th BD-to-LR link, respectively; $n_p \sim \mathcal{CN}(0,\sigma^2)$ is the AWGN at the LR. Thus the SINR at the LR is written as

$$\gamma_k^{(1)} = \frac{P_t K_p |h_p|^2}{\eta_k (1-\beta_k) P_t K_{1k} K_k^s |h_{1k}|^2 |g_k^s|^2 + \sigma^2}. \quad (6)$$

(ii) If $E_k < P_{c,k}T$, the k-th BD keeps silent and the k-th BR link is in outage. In this case, the received signal at the LR is written as

$$y_k^{(2)} = \sqrt{P_t K_p} h_p x_p + n_p. \quad (7)$$

Then the signal-to-noise-ratio (SNR) at the LR is calculated as

$$\gamma_k^{(2)} = \frac{P_t K_p |h_p|^2}{\sigma^2}. \quad (8)$$

III. Outage Analysis for AmBackComs

In this section, we analyze the outage performance[2] for the considered backscatter system. Assume that the k-th BD is selected to backscatter information to its receiver, while other backscatter links keep silent. Let $\mathcal{P}_{\text{out},k}^b$ denote the outage

---

[2]Reliable transmission and the performance evaluation are crucially important in wireless communication systems. The outage probability has been recognized as one of important performance metrics to evaluate the reliability of a transmission link, since it provides a lowest bound on the transmission error probability [35].

---

probability for the k-th backscatter link. For a given SINR threshold γ_{th}^b, $\mathcal{P}_{\text{out},k}^b$ can be calculated as

$$\mathcal{P}_{\text{out},k}^b = \mathbb{P}(E_k < P_{c,k}T) + \mathbb{P}(\gamma_k^b < \gamma_{\text{th}}^b, E_k \geq P_{c,k}T), \quad (9)$$

where the first term denotes the energy outage probability that the k-th BD does not have enough energy for backscattering while the second term expresses the probability that the k-th BR fails to decode backscattered information in the case of $E_k \geq P_{c,k}T$.

A. Adaptive RC Scheme

For the backscatter link, we adopt an adaptive RC scheme to minimize the outage probability of the backscatter link. Since minimizing the outage probability $\mathcal{P}_{\text{out},k}^b$ is equivalent to maximizing the successful transmission probability for the backscatter link and the successful transmission happens only when $\gamma_k^b \geq \gamma_{\text{th}}^b$ and $E_k \geq P_{c,k}T$ hold simultaneously, we can formulate the optimization problem as

$$\mathbf{P}_1: \max_{\beta_k} \mathbb{P}(\gamma_k^b \geq \gamma_{\text{th}}^b)$$
$$\text{s.t. C1}: E_k \geq P_{c,k}T,$$
$$\text{C2}: 0 \leq \beta_k \leq 1,$$

where constraint C1 should be satisfied to ensure that the harvested energy is enough for circuit operation consumption during backscattering. It is worth noting that for the case with $E_k < P_{c,k}T$, $\mathcal{P}_{\text{out},k}^b$ is always equal to 1 since the k-th BD is always inactive due to the lack of energy.

After some mathematical calculations, the problem $\mathbf{P}_1$ can be transformed as

$$\mathbf{P}_2: \max_{\beta_k} \mathbb{P}(\gamma_k^b \geq \gamma_{\text{th}}^b)$$
$$\text{s.t.}: \min\left(\frac{\Phi_k}{P_t K_{1k}|h_{1k}|^2}, 1\right) \leq \beta_k \leq 1,$$

where $\Phi_k = \frac{\ln \frac{E_{\max,k} e^{s_{1k} s_{0k}} + P_{c,k} e^{s_{1k} s_{2k}}}{E_{\max,k} - P_{c,k}}}{s_{1k}}$.

Proof. Substituting (2) into constraint C1 and after some mathematical manipulation, we have $P_{r,k} \geq \Phi_k$. As $P_{r,k} = \beta_k P_t K_{1k} |h_{1k}|^2$ denotes the received power at the k-th BD, we can derive the following inequality, i.e., $\beta_k \geq \frac{\Phi_k}{P_t K_{1k}|h_{1k}|^2}$. Since $E_{\max,k} > P_{c,k}$, $\beta_k > 0$ always holds. Combining $\beta_k \geq \frac{\Phi_k}{s_{1k} P_t K_{1k}|h_{1k}|^2}$ with constraint C2, we obtain the range of β_k as $\min\left(\frac{\Phi_k}{P_t K_{1k}|h_{1k}|^2}, 1\right) \leq \beta_k \leq 1$. $\blacksquare$

Since $\mathbb{P}(\gamma_k^b \geq \gamma_{\text{th}}^b)$ decreases with the increasing of β_k, the optimal RC for the k-th BD is given by

$$\beta_k^* = \min\left(\frac{\Phi_k}{P_t K_{1k}|h_{1k}|^2}, 1\right). \quad (10)$$

The derived expression in (10) provides a guideline to set the value of RC in a practical AmBackCom.

$$\mathcal{P}_{\text{out},k}^{\text{HS}} \approx 1 - \exp\left(-\frac{b_k}{a_k\lambda_{1k}}\right)\left[1 - F_{S_k}\left(\gamma_{\text{th}}^b\sigma^2\right) - \exp\left(\frac{\sigma^2}{P_tK_k^p\lambda_k^p}\right)\left[\Theta_k - \frac{1}{\lambda_{1k}\lambda_{2k}a_k}\left(\frac{\gamma_{\text{th}}^b\sigma^4}{P_tK_k^p\lambda_k^p}\left(\ln\left(\frac{\sqrt{\gamma_{\text{th}}^b}\sigma}{\sqrt{\lambda_{1k}\lambda_{2k}a_k}}\right) - \frac{1}{4}\right)\right.\right.$$

$$\left.\left. - 2\gamma_{\text{th}}^b\sigma^2\left(\ln\left(\frac{\sqrt{\gamma_{\text{th}}^b}\sigma}{\sqrt{\lambda_{1k}\lambda_{2k}a_k}}\right) - \frac{1}{2}\right)\right) + 2\gamma_{\text{th}}^b\vartheta_kc_0\left(1 - \exp\left(-\frac{\sigma^2}{P_tK_k^p\lambda_k^p}\right)\right)\right]\right]. \quad (16)$$

B. Outage Analysis for the k-th Backscatter Link

By applying β_k^*, $\mathcal{P}_{\text{out},k}^b$ can be rewritten as

$$\mathcal{P}_{\text{out},k}^b = \underbrace{\mathbb{P}\left(|h_{1k}|^2 < \frac{b_k}{a_k}\right)}_{I_1}$$
$$+ \underbrace{\mathbb{P}\left(\frac{S_k}{P_tK_k^p|g_k^p|^2 + \sigma^2} < \gamma_{\text{th}}^b, |h_{1k}|^2 \geq \frac{b_k}{a_k}\right)}_{I_2}, \quad (11)$$

where $a_k = \eta_kP_tK_{1k}K_{2k}$, $b_k = \eta_k\Phi_kK_{2k}$, and $S_k = \begin{cases} a_k|h_{1k}|^2|h_{2k}|^2 - b_k|h_{2k}|^2, & \text{if } |h_{1k}|^2 \geq \frac{b_k}{a_k} \\ 0, & \text{otherwise} \end{cases}$.

Since the multiplicative and additive channel gain, S_k, is included in (11), we first provide a proposition to derive its probability density function (PDF) and then calculate the outage probability of k-th backscatter link in the following context.

Proposition 1: Based on $|h_{2k}|^2 \sim \exp(\frac{1}{\lambda_{2k}})$, conditioning on $|h_{1k}|^2 \geq \frac{b_k}{a_k}$, the cumulative distribution function (CDF) of S_k, denoted by $F_{S_k}(x)$, and the PDF of S_k, denoted by $f_{S_k}(x)$, are, respectively, given by

$$F_{S_k}(x) = 1 - \frac{1}{\lambda_{1k}a_k}\sqrt{\frac{4a_k\lambda_{1k}x}{\lambda_{2k}}}K_1\left(\sqrt{\frac{4x}{\lambda_{2k}\lambda_{1k}a_k}}\right), \quad (12)$$

$$f_{S_k}(x) = \frac{2}{\lambda_{1k}\lambda_{2k}a_k}K_0\left(2\sqrt{\frac{x}{\lambda_{1k}\lambda_{2k}a_k}}\right), \quad (13)$$

where both $K_0(\cdot)$ are $K_1(\cdot)$ are the modified Bessel functions of the second kind [36].

Proof: See Appendix A. ∎

Using Proposition 1, we can obtain the following theorem.

Theorem 1. The outage probability of the k-th backscatter link can be calculated as

$$\mathcal{P}_{\text{out},k}^b =$$
$$1 - \exp\left(-\frac{b_k}{a_k\lambda_{1k}}\right)\left[1 - F_{S_k}\left(\gamma_{\text{th}}^b\sigma^2\right) - \exp\left(\frac{\sigma^2}{P_tK_k^p\lambda_k^p}\right)\right.$$
$$\left.\times\left(\Theta_k - \int_0^{\gamma_{\text{th}}^b\sigma^2}\exp\left(-\frac{x}{\gamma_{\text{th}}^bP_tK_k^p\lambda_k^p}\right)f_{S_k}(x)\,dx\right)\right], \quad (14)$$

where $\Theta_k = -\vartheta_k\gamma_{\text{th}}^b\text{Ei}(-\vartheta_k\gamma_{\text{th}}^b)\exp\left(\vartheta_k\gamma_{\text{th}}^b\right)$ with $\vartheta_k = \frac{P_tK_k^p\lambda_k^p}{\lambda_{1k}\lambda_{2k}a_k}$ and the exponential integral function $\text{Ei}(\varrho) = \int_{-\infty}^\varrho t^{-1}e^t dt$ [eq. (8.211.1), [36]].

Proof: See Appendix B. ∎

Although (14) is more analytical than (11), there is still no closed-form expression for $\mathcal{P}_{\text{out},k}^b$ due to the involved integral $\int_0^{\gamma_{\text{th}}^b\sigma^2}\exp\left(-\frac{x}{\gamma_{\text{th}}^bP_tK_k^p\lambda_k^p}\right)f_{S_k}(x)\,dx$. In what follows, we provide two ways to address this problem. One is to use Gaussian-Chebyshev quadrature to obtain an approximation for $\mathcal{P}_{\text{out},k}^b$ for any given P_t, since it can provide sufficient level of accuracy within very few terms [34], [37], [38]. The other is to approximate $\mathcal{P}_{\text{out},k}^b$ based on a high transmit power of the LT. Such an approach aims to find some insights and has been widely used in the field of performance analysis.

Gaussian-Chebyshev Approximation: Based on the Gaussian-Chebyshev quadrature, we have the following approximation, i.e.,

$$\mathcal{P}_{\text{out},k}^b \approx 1 - \exp\left(-\frac{b_k}{a_k\lambda_{1k}}\right)$$
$$\times\left[1 - F_{S_k}\left(\gamma_{\text{th}}^b\sigma^2\right) - \exp\left(\frac{\sigma^2}{P_tK_k^p\lambda_k^p}\right)\right.$$
$$\times\left(\Theta_k - \frac{\pi\gamma_{\text{th}}^b\sigma^2}{2M}\sum_{m=1}^M\sqrt{1 - v_m^2}\right.$$
$$\left.\left.\times\exp\left(-\frac{\kappa_m^{(0)}}{\gamma_{\text{th}}^bP_tK_k^p\lambda_k^p}\right)f_{S_k}\left(\kappa_m^{(0)}\right)\right)\right], \quad (15)$$

where $v_m = \cos\frac{2m-1}{2M}\pi$, $\kappa_m^{(0)} = \frac{\gamma_{\text{th}}^b\sigma^2}{2}v_m + \frac{\gamma_{\text{th}}^b\sigma^2}{2}$, and M is a parameter that determines the tradeoff between complexity and accuracy.

Remark 1: The derived expression in (15) has the following applications. Firstly, it provides a closed-form expression that can accurately evaluate the outage probability of the k-th backscatter link with a small M, thus avoiding the necessity of Monte Carlo simulations. This would be useful for the service providers and the industry, who may take up experiments and/or implementations based on their assessments of the reported results, because they need to know the bound performance of a practical system. Secondly, the outage probability expression in (15) and the numerical results generated using it enable us to obtain useful insights into how the system parameters affect the outage performance of a backscatter system.

Outage Probability with a High Transmit Power of the LT: Assuming a high transmit power of the LT, we derive the outage probability for the k-th backscatter link, denoted by $\mathcal{P}_{\text{out},k}^{\text{HS}}$, which is given (16), as shown at the top of the next page.

Proof: See Appendix D. ∎

Using (16), we can see that $\mathcal{P}_{\text{out},k}^{\text{HS}}$ converges to a lower bound when $P_t \to \infty$, given by

$$\lim_{P_t \to \infty} \mathcal{P}_{\text{out},k}^{\text{HS}} = -\frac{K_k^p \lambda_k^p \gamma_{\text{th}}^b}{\lambda_{1k} \lambda_{2k} \eta_k K_{1k} K_{2k}} \text{Ei}\left(-\frac{K_k^p \lambda_k^p \gamma_{\text{th}}^b}{\lambda_{1k} \lambda_{2k} \eta_k K_{1k} K_{2k}}\right)$$
$$\times \exp\left(\frac{K_k^p \lambda_k^p \gamma_{\text{th}}^b}{\lambda_{1k} \lambda_{2k} \eta_k K_{1k} K_{2k}}\right). \quad (17)$$

Proof: If $P_t \to \infty$, ϑ_k is bound and a_k converges to infinity. Thus, $\exp\left(-\frac{b_k}{a_k \lambda_{1k}}\right)$, $F_{S_k}\left(\gamma_{\text{th}}^b \sigma^2\right)$, $\exp\left(\frac{\sigma^2}{P_t K_k^p \lambda_k^p}\right)$ and $\exp\left(-\frac{\sigma^2}{P_t K_k^p \lambda_k^p}\right)$ converge to one. Combing this conclusion, i.e., $\lim_{a_k \to \infty} \frac{\ln\left(\frac{\sqrt{\gamma_{\text{th}}^b}\sigma}{\sqrt{\lambda_{1k} \lambda_{2k} a_k}}\right)}{\lambda_{1k} \lambda_{2k} a_k} = \lim_{a_k \to \infty} \frac{-\frac{1}{2a_k}}{\lambda_{1k} \lambda_{2k}} = 0$, (17) can be obtained. ∎

Remark 2: The bound in (17) reveals that the interference caused by the legacy transmission leads to the outage saturation phenomenon of the k-th backscatter link, and that the diversity gain of the k-th backscatter link can be calculated as $\lim_{P_t \to \infty} -\frac{\log\left(\mathcal{P}_{\text{out},k}^{\text{HS}}\right)}{\log P_t} = 0$. This is because the interference link from the LT-to-the k-th BR scales along the transmit power of the LT at each block, which leads to a bound of γ_k^b as P_t grows. Also, it reveals that how the channel qualities impact on the low bound for the outage probability of the k-th backscatter link. In particular, $\lim_{P_t \to \infty} \mathcal{P}_{\text{out},k}^{\text{HS}}$ decreases with the increase of $\frac{K_k^p \lambda_k^p}{\lambda_{1k} \lambda_{2k} K_{1k} K_{2k}}$ that is related with the means of the channel gains of the LT-to-the k-th BD link, the k-th backscatter link and the interfering link from LT-to-BR.

To better understand the performance bounds of backscatter systems, we turn our attention to investigate its outage probability under two extreme cases.

1) Outage Probability under the Best Case: Specifically, the selected backscatter link with the maximum SINR at the BR results in the best case. Denote the outage probability of this case as $\mathcal{P}_{\text{out},b}^{\text{bc}}$, which can be computed as

$$\mathcal{P}_{\text{out},b}^{\text{bc}} = \mathbb{P}\left(\max\left(\frac{S_1}{P_t K_{r1}|g_1^p|^2 + \sigma^2}, \ldots, \frac{S_K}{P_t K_{rK}|g_K^p|^2 + \sigma^2}\right) < \gamma_{\text{th}}^b\right)$$
$$\overset{(a)}{=} \prod_{k=1}^{K} \mathbb{P}\left(\frac{S_k}{P_t K_k^p |g_k^p|^2 + \sigma^2} < \gamma_{\text{th}}^b\right)$$
$$= \prod_{k=1}^{K} \mathcal{P}_{\text{out},k}^b, \quad (18)$$

where step (a) holds since $\left\{\frac{S_k}{P_t K_k^p |g_k^p|^2 + \sigma^2}\right\}_{k \in \{1,\ldots,K\}}$ are independent of each other.

Accordingly, the lower bound of the outage probability for this case is given as

$$\lim_{P_t \to \infty} \mathcal{P}_{\text{out},b}^{\text{bc}} = \prod_{k=1}^{K} \lim_{P_t \to \infty} \mathcal{P}_{\text{out},k}^{\text{HS}}. \quad (19)$$

2) Outage Probability under the Worst Case: The worst case will happen when the selected backscatter link achieves the minimum SINR at the BR. Under such case, the outage probability, denoted by $\mathcal{P}_{\text{out},b}^{\text{wc}}$, is given by

$$\mathcal{P}_{\text{out},b}^{\text{wc}}$$
$$= \mathbb{P}\left(\min\left(\frac{S_1}{P_t K_{r1}|g_1^p|^2 + \sigma^2}, \ldots, \frac{S_K}{P_t K_{rK}|g_K^p|^2 + \sigma^2}\right) < \gamma_{\text{th}}^b\right)$$
$$= 1 - \mathbb{P}\left(\min\left(\frac{S_1}{P_t K_{r1}|g_1^p|^2 + \sigma^2}, \ldots, \frac{S_K}{P_t K_{rK}|g_K^p|^2 + \sigma^2}\right) \geq \gamma_{\text{th}}^b\right)$$
$$= 1 - \prod_{k=1}^{K} \left(\frac{S_k}{P_t K_k^p |g_k^p|^2 + \sigma^2} \geq \gamma_{\text{th}}^b\right)$$
$$= 1 - \prod_{k=1}^{K} \left(1 - \mathcal{P}_{\text{out},k}^b\right). \quad (20)$$

Similarly as (19), the low bound of the outage probability in the worst case for the backscatter system is written as

$$\lim_{P_t \to \infty} \mathcal{P}_{\text{out},b}^{\text{wc}} = 1 - \prod_{k=1}^{K} \left(1 - \lim_{P_t \to \infty} \mathcal{P}_{\text{out},k}^{\text{HS}}\right). \quad (21)$$

IV. OUTAGE ANALYSIS FOR LEGACY TRANSMISSION

In this section, we study the outage performance of the legacy system in order to see how backscatter system influences the legacy transmission. For the legacy transmission with a given backscatter link, an outage event will occur in two cases. The first case is that the BD does not have enough energy for backscattering while the received SNR at the LR is less than the given threshold. The second case is that the BD has enough energy for backscattering while the received SINR at the LR is less than the given threshold. Let $\mathcal{P}_{\text{out},k}^l$ denote the outage probability for the legacy link when the k-th backscatter link is selected. Let γ_{th} be the threshold for the legacy transmission. Then $\mathcal{P}_{\text{out},k}^l$ is given by

$$\mathcal{P}_{\text{out},k}^l = \mathbb{P}(\gamma_k^{(1)} < \gamma_{\text{th}}, E_k \geq P_{c,k}T)$$
$$+ \mathbb{P}(\gamma_k^{(2)} < \gamma_{\text{th}}, E_k < P_{c,k}T), \quad (22)$$

where the first term and the second term denote the outage probabilities for the cases with $E_k \geq P_{c,k}T$ and $E_k < P_{c,k}T$, respectively.

Considering β_k^*, $\mathcal{P}_{\text{out},k}^l$ can be rewritten as

$$\mathcal{P}_{\text{out},k}^l = \underbrace{\mathbb{P}\left(\frac{P_t K_p |h_p|^2}{\sigma^2} < \gamma_{\text{th}}, |h_{1k}|^2 < \frac{b_k}{a_k}\right)}_{I_3}$$
$$+ \underbrace{\mathbb{P}\left(\frac{P_t K_p |h_p|^2}{G_k + \sigma^2} < \gamma_{\text{th}}, |h_{1k}|^2 \geq \frac{b_k}{a_k}\right)}_{I_4}, \quad (23)$$

where $a_{ik} = \eta_k P_t K_{1k} K_k^s$, $b_{ik} = \eta_k \Phi_k K_k^s$, and $G_k = \begin{cases} a_{ik}|h_{1k}|^2 |g_k^s|^2 - b_{ik}|g_k^s|^2, & \text{if } |h_{1k}|^2 \geq \frac{b_k}{a_k} \\ 0, & \text{otherwise} \end{cases}$.

Since both $|h_p|^2$ and $|h_{1k}|^2$ are independent of each other, I_3 can be calculated as

$$
I_3 = \mathbb{P}\left(\frac{P_t K_p |h_p|^2}{\sigma^2} < \gamma_{\text{th}}\right) \mathbb{P}\left(|h_{1k}|^2 < \frac{b_k}{a_k}\right)
$$

$$
= \left(1 - \exp\left(-\frac{\gamma_{\text{th}}\sigma^2}{P_t K_p \lambda_p}\right)\right)\left(1 - \exp\left(-\frac{b_k}{\lambda_{1k} a_k}\right)\right). \quad (24)
$$

Similarly to the derivation in Appendix B, I_4 can be written as

$$
I_4 = \mathbb{P}\left(|h_p|^2 < \frac{\gamma_{\text{th}}(G_k + \sigma^2)}{P_t K_p}\bigg||h_{1k}|^2 \geq \frac{b_k}{a_k}\right)\mathbb{P}\left(|h_{1k}|^2 \geq \frac{b_k}{a_k}\right)
$$

$$
= \exp\left(-\frac{b_k}{a_k \lambda_{1k}}\right)\left[1 - \exp\left(-\frac{\gamma_{\text{th}}\sigma^2}{P_t K_p \lambda_p}\right)I_5\right], \quad (25)
$$

where $I_5 = \int_0^{+\infty} \exp\left(-\frac{\gamma_{\text{th}} x}{P_t K_p \lambda_p}\right) f_{G_k}(x)\, dx$ and $f_{G_k}(x)$ denotes the PDF of G_k under the case of $|h_{1k}|^2 \geq \frac{b_k}{a_k}$.

Similarly as Proposition 1, we have $f_{G_k}(x) = \frac{2}{\lambda_{1k}\lambda_k^s a_{ik}}K_0\left(2\sqrt{\frac{x}{\lambda_{1k}\lambda_k^s a_{ik}}}\right)$. Based on Appendix C, I_5 can be computed as

$$
I_5 = -\Xi_k \exp(\Xi_k) \operatorname{Ei}(-\Xi_k), \quad (26)
$$

where $\Xi_k = \frac{P_t K_p \lambda_p}{\gamma_{\text{th}}\lambda_{1k}\lambda_k^s a_{ik}}$.

Substituting (24), (25) and (26) into (23), $\mathcal{P}_{\text{out},k}^l$ is obtained. Then we can obtain the lower bound for the outage probability of the legacy transmission, given by

$$
\lim_{P_t \to \infty} \mathcal{P}_{\text{out},k}^l = 1 + \frac{K_p \lambda_p}{\eta_k \gamma_{\text{th}}\lambda_{1k}\lambda_k^s K_{1k}K_k^s} \times
$$

$$
\exp\left(\frac{K_p \lambda_p}{\eta_k \gamma_{\text{th}}\lambda_{1k}\lambda_k^s K_{1k}K_k^s}\right)\operatorname{Ei}\left(-\frac{K_p \lambda_p}{\eta_k \gamma_{\text{th}}\lambda_{1k}\lambda_k^s K_{1k}K_k^s}\right). \quad (27)
$$

In the following, we will further analyze the outage probability for the legacy transmission under two extreme cases so that we can know the bound performance of the legacy transmission. The first case (also termed as best case) is caused by the selected backscatter link with the minimum interference on the LR and will lead to the lowest outage probability of the legacy transmission. The second case is the worst case, where the selected backscatter link results in the maximum interference on the LR.

A. Outage Probability under the Best Case

There are two cases for the outage probability under the best case. Specifically, when there is at least one backscatter link that is inactive due to the lack of energy, the best case for the legacy transmission happens with the inactive backscatter link selected. In this case, the received SNR at the LR is given by $\gamma_k^{(2)}$. When all the backscatter links have enough energy for backscattering, the backscatter link with the minimum interference $G_{\min} = \min\{G_1, G_2, \cdots, G_K\}$ should be selected and the received SINR is determined by $\gamma_{\text{bc}}^l = \frac{P_t K_p |h_p|^2}{G_{\min} + \sigma^2}$. Accordingly, we can compute the outage probability under the best case as

$$
\mathcal{P}_{\text{out},l}^{\text{bc}} = \mathcal{P}_{\text{out},l}^{\text{No-SL}}(1 - \mathcal{P}_1) + \mathcal{P}_2 \mathcal{P}_1, \quad (28)
$$

where $\mathcal{P}_1$ is the probability that all the backscatter links have enough energy for backscattering; $\mathcal{P}_2$ is the probability of $\gamma_{\text{bc}}^l < \gamma_{\text{th}}$ conditioning on all active backscatter links, and $\mathcal{P}_{\text{out},l}^{\text{No-SL}}$ is the outage probability of the legacy transmission when the backscatter link is inactive, i.e., the backscatter link has no impacts on the legacy transmission. $\mathcal{P}_{\text{out},l}^{\text{No-SL}}$ is given by

$$
\mathcal{P}_{\text{out},l}^{\text{No-SL}} = \mathbb{P}\left(\frac{P_t K_p |h_p|^2}{\sigma^2} < \gamma_{\text{th}}\right)
$$

$$
= 1 - \exp\left(-\frac{\gamma_{\text{th}}\sigma^2}{P_t K_p \lambda_p}\right). \quad (29)
$$

Thus, in order to obtain the value of $\mathcal{P}_{\text{out},l}^{\text{bc}}$, we should determine the values of $\mathcal{P}_1$ and $\mathcal{P}_2$ first. Based on the definitions, $\mathcal{P}_1$ can be calculated as

$$
\mathcal{P}_1 = \mathbb{P}\left(\bigcap_{k=1}^{K} |h_{1k}|^2 > \frac{b_k}{a_k}\right) = \prod_{k=1}^{K} \exp\left(-\frac{b_k}{\lambda_{1k} a_k}\right). \quad (30)
$$

$\mathcal{P}_2$ is determined by

$$
\mathcal{P}_2 = \mathbb{P}\left(\gamma_{\text{bc}}^l < \gamma_{\text{th}}\bigg|\bigcap_{k=1}^{K} |h_{1k}|^2 > \frac{b_k}{a_k}\right)
$$

$$
= 1 - \exp\left(-\frac{\gamma_{\text{th}}\sigma^2}{P_t K_p \lambda_p}\right)
$$

$$
\times \mathbb{E}\left[\exp\left(-\frac{\gamma_{\text{th}}G_{\min}}{P_t K_p \lambda_p}\right)\bigg|\bigcap_{k=1}^{K} |h_{1k}|^2 > \frac{b_k}{a_k}\right]. \quad (31)
$$

Proposition 2: The CDF of $\min(G_1, G_2, \ldots, G_K)$ conditioned on $\bigcap_{k=1}^{K} |h_{1k}|^2 > \frac{b_k}{a_k}$, denoted by $F_{G_{\min}}(x)$, is given by

$$
F_{G_{\min}}(x)
$$

$$
= 1 - \prod_{k=1}^{K}\left[\frac{1}{\lambda_{1k}a_{ik}}\sqrt{\frac{4a_{ik}\lambda_{1k}x}{\lambda_k^s}}K_1\left(\sqrt{\frac{4x}{\lambda_{1k}\lambda_k^s a_{ik}}}\right)\right]. \quad (32)
$$

Proof: See Appendix E. ∎

According to the Proposition 2, $\mathcal{P}_2$ can be computed as

$$
\mathcal{P}_2
$$

$$
= 1 - \exp\left(-\frac{\gamma_{\text{th}}\sigma^2}{P_t K_p \lambda_p}\right)\int_0^{+\infty} \exp\left(-\frac{\gamma_{\text{th}} x}{P_t K_p \lambda_p}\right)f_{G_{\min}}(x)dx
$$

$$
\stackrel{(a)}{=} 1 - e^{-\frac{\gamma_{\text{th}}\sigma^2}{P_t K_p \lambda_p}}\int_0^{+\infty} \exp(-t)F_{G_{\min}}\left(\frac{P_t K_p \lambda_p t}{\gamma_{\text{th}}}\right)dt
$$

$$
\stackrel{(b)}{=} 1 - e^{-\frac{\gamma_{\text{th}}\sigma^2}{P_t K_p \lambda_p}}\int_0^{1} F_{G_{\min}}\left(-\frac{P_t K_p \lambda_p}{\gamma_{\text{th}}}\ln y\right)dy, \quad (33)
$$

where $f_{G_{\min}}(x)$ is the PDF of $G_{\min}$ conditioned on $\bigcap_{k=1}^{K} |h_{1k}|^2 > \frac{b_k}{a_k}$; step (a) follows by using the subsection integral method and letting $t = \frac{\gamma_{\text{th}} x}{P_t K_p \lambda_p}$; step (b) holds by letting $y = e^{-t}$.
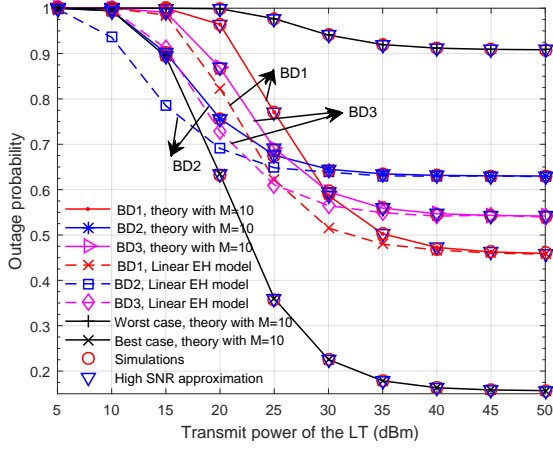
Fig. 2. Outage probability for a backscatter system versus the transmit power of the LT.

Fig. 3. Outage capacity for the third backscatter link versus the circuit power consumption.

Similar to (15), we employ Gaussian-Chebyshev quadrature to obtain an approximation for $\mathcal{P}_2$, given by

$$
\begin{aligned}
\mathcal{P}_2 \approx 1 &- \frac{\pi e^{-\frac{\gamma_{\mathrm{th}}\sigma^2}{P_t K_p \lambda_p}}}{2M} \\
&\times \sum_{m=1}^{M} \sqrt{1-v_m^2}\, F_{G_{\min}}\left(-\frac{P_t K_p \lambda_p}{\gamma_{\mathrm{th}}}\ln\kappa_m^{(1)}\right), \quad (34)
\end{aligned}
$$

where $\kappa_m^{(1)} = \frac{v_m}{2} + \frac{1}{2}$.

Based on (28), (29), (30) and (34), $\mathcal{P}_{\mathrm{out},l}^{\mathrm{bc}}$ can be obtained. Accordingly, the lower bound for the outage probability of the legacy transmission in the best case can be written as

$$
\begin{aligned}
\lim_{P_t \to \infty} \mathcal{P}_{\mathrm{out},l}^{\mathrm{bc}} \approx 1 &- \frac{\pi}{2M}\sum_{m=1}^{M}\sqrt{1-v_m^2} \\
&\times F_{G_{\min}}\left(-\frac{P_t K_p \lambda_p}{\gamma_{\mathrm{th}}}\ln\kappa_m^{(1)}\right). \quad (35)
\end{aligned}
$$

B. Outage Probability under the Worst Case

Likewise, the outage probability under the worst case is given by

$$
\begin{aligned}
&\mathcal{P}_{\mathrm{out},l}^{\mathrm{wc}} \\
&= 1-\exp\left(-\frac{\gamma_{\mathrm{th}}\sigma^2}{P_t K_p \lambda_p}\right)\mathbb{E}\left[\exp\left(-\frac{\gamma_{\mathrm{th}}\widehat{G}_{\max}}{P_t K_p \lambda_p}\right)\right] \\
&= 1-\exp\left(-\frac{\gamma_{\mathrm{th}}\sigma^2}{P_t K_p \lambda_p}\right)\int_0^{+\infty}\exp\left(-\frac{\gamma_{\mathrm{th}}x}{P_t K_p \lambda_p}\right)f_{\widehat{G}_{\max}}(x)\,dx \\
&= 1-\exp\left(-\frac{\gamma_{\mathrm{th}}\sigma^2}{P_t K_p \lambda_p}\right)\int_0^1 F_{\widehat{G}_{\max}}\left(-\frac{P_t K_p \lambda_p}{\gamma_{\mathrm{th}}}\ln t\right)dt, \quad (36)
\end{aligned}
$$

where $\widehat{G}_{\max} = \max\{\widehat{G}_1, \widehat{G}_2, \cdots, \widehat{G}_K\}$ with $\widehat{G}_k = \begin{cases} G_k, & |h_{1k}|^2 > \frac{b_k}{a_k} \\ 0, & |h_{1k}|^2 \le \frac{b_k}{a_k} \end{cases}$, $f_{\widehat{G}_{\max}}(x)$ denotes the PDF of $\widehat{G}_{\max}$ and $F_{\widehat{G}_{\max}}(x)$ is the CDF of $\widehat{G}_{\max}$.
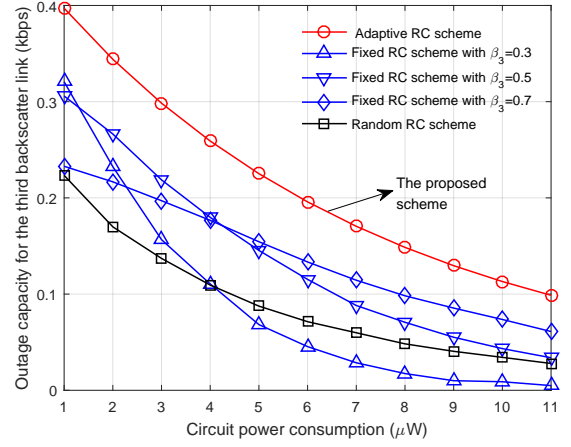
Table II Meaning of the Derived Outage Probabilities

Notation	Meaning
$\mathcal{P}_{\mathrm{out},k}^{b}$	Outage probability for the k-th backscatter link
$\mathcal{P}_{\mathrm{out},b}^{\mathrm{bc}}$	The lowest outage probability for the backscatter system
$\mathcal{P}_{\mathrm{out},b}^{\mathrm{wc}}$	The highest outage probability for the backscatter system
$\mathcal{P}_{\mathrm{out},k}^{l}$	Outage probability for the legacy link when the k-th backscatter link is selected
$\mathcal{P}_{\mathrm{out},l}^{\mathrm{bc}}$	The lowest outage probability for the legacy system
$\mathcal{P}_{\mathrm{out},l}^{\mathrm{wc}}$	The highest outage probability for the legacy system

Proposition 3: The CDF of $\max\{\widehat{G}_1, \widehat{G}_2, \cdots, \widehat{G}_K\}$, denoted by $F_{\widehat{G}_{\max}}(x)$, is given by

$$
\begin{aligned}
&F_{\widehat{G}_{\max}}(x) \\
&= \prod_{k=1}^{K}\left(1 - \frac{1}{\lambda_{1k}a_{ik}}\sqrt{\frac{4a_{ik}\lambda_{1k}x}{\lambda_k^s}}K_1\left(\sqrt{\frac{4x}{\lambda_{1k}\lambda_k^s a_{ik}}}\right)\right) \\
&\quad \times \exp\left(-\frac{b_k}{a_k\lambda_{1k}}\right) + 1 - \exp\left(-\frac{b_k}{a_k\lambda_{1k}}\right). \quad (37)
\end{aligned}
$$

Proof: See Appendix F. ∎

Based on the Proposition 3, by using Gaussian-Chebyshev quadrature, $\mathcal{P}_{\mathrm{out},l}^{\mathrm{wc}}$ can be approximated as

$$
\begin{aligned}
\mathcal{P}_{\mathrm{out},l}^{\mathrm{wc}} \approx 1 &- \frac{\pi e^{-\frac{\gamma_{\mathrm{th}}\sigma^2}{P_t K_p \lambda_p}}}{2M} \\
&\times \sum_{m=1}^{M}\sqrt{1-v_m^2}\, F_{\widehat{G}_{\max}}\left(-\frac{P_t K_p \lambda_p}{\gamma_{\mathrm{th}}}\ln\kappa_m^{(1)}\right). \quad (38)
\end{aligned}
$$

Thus the low bound for the outage probability of the legacy transmission in the worst case can be computed as

$$
\begin{aligned}
\lim_{P_t \to \infty}\mathcal{P}_{\mathrm{out},l}^{\mathrm{wc}} \approx 1 &- \frac{\pi}{2M}\sum_{m=1}^{M}\sqrt{1-v_m^2} \\
&\times F_{\widehat{G}_{\max}}\left(-\frac{P_t K_p \lambda_p}{\gamma_{\mathrm{th}}}\ln\kappa_m^{(1)}\right). \quad (39)
\end{aligned}
$$

For better understanding, we summarize the meaning of the derived outage probabilities as Table II.
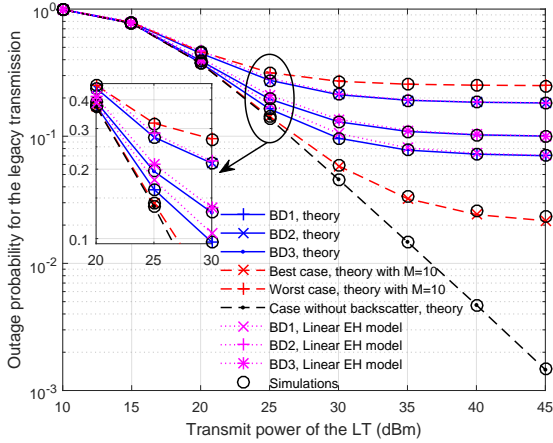
Fig. 4. Outage probability of the legacy transmission versus the transmit power of the LT.

Fig. 5. Outage probability of the legacy transmission versus the given transmission rate.

V. SIMULATION AND DISCUSSION

In this section, we evaluate the outage performance of AmBackComs. In what follows, based on [15]–[17], [29], we set the basic parameter values as follows: $K = 3$, $W = 1$ MHz, $T = 1$ second, $P_{c,1} = P_{c,2} = P_{c,3} = 8.9$ μW, $U = 1$ kbps, and $\alpha = 2.7$. The backscatter efficiency η_k reflects a loss of 1.1 dB [15], and the noise power spectral density is set to be -120 dBm/Hz [29]. For the legacy transmission, the given transmission rate is set as 10 Mbps. According to [32], the parameters of the considered non-linear EH model is set as $E_{\max,1} = E_{\max,2} = E_{\max,3} = 240\mu$W, $s_{11} = s_{12} = s_{13} = 5000$ and $s_{21} = s_{22} = s_{23} = 0.0002$.

Besides the above simulation parameters, the distances are set as: $d_p = 10$ metres, $d_1^p = 5$ metres, $d_2^p = 3$ metres, $d_3^p = 4$ metres, $d_{11} = 4$ metres, $d_{12} = 2$ metres, $d_{13} = 3$ metres, $d_{21} = 1.2$ metres, $d_{22} = 2$ metres, $d_{23} = 1.5$ metres, $d_1^s = 7$ metres, $d_2^s = 9$ metres, and $d_3^s = 8$ metres. According to [34], we suppose that the LT transmits its signal at 915 MHz and the antenna gain for each BD is set to be 1.8 dBi, while the antenna gains for the LT, the LR and the BRs are all set as 6 dBi.

A. Outage performance analysis for the backscatter links

Fig. 2 shows the outage probabilities of the backscatter system versus the transmit power of the LT P_t. Note that the outage probability for the k-th ($k \in \{1, 2, 3\}$) backscatter link is computed based on (15) ((16) for the high SNR approximation) while the outage probabilities under the best case and the worst case are determined by (18) and (20), respectively. For the linear EH model, the conversion efficiency is fixed as 0.8 throughout the simulations. As shown in this figure, we can see that our derived analytical results match well with simulation results that are obtained by over 1×10^6 Monte Carlo simulations and marked by red circles. This observation demonstrates the correctness of our derived outage probabilities. It also shows that a small M, i.e., $M = 10$, is sufficient to provide an accurate outage probability for Gaussian-Chebyshev approximation. Besides, the outage probabilities under the linear EH model can not correctly
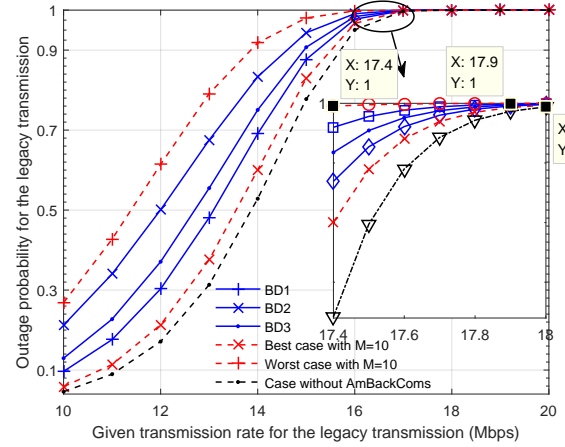
characterize the outage performance of the backscatter system. For example, the outage performance under the linear model is over-estimated for the backscatter system. In addition, we can also observe that all the outage probabilities decrease with the increasing of P_t and when P_t is large enough, all the outage probabilities get saturated. That is to say, there exists an error floor caused by the interference from the legacy transmission. Another observation is that the outage probability under the best case can achieve the best outage performance while the outage probability under the worst case is the highest as expected. It is also found that choosing the backscatter link with the maximum SINR at the BR for backscattering can greatly reduce the error floor and improve the outage performance of backscatter system.

Fig. 3 illustrates the outage capacity for the backscatter link versus the circuit power consumption, where the third BD is selected to backscatter information and three schemes are employed at the BD, namely the proposed adaptive RC scheme, the fixed RC scheme and the random RC scheme. Specifically, P_t is set to be 20 dBm. For the proposed scheme, the RC ratio is determined by (10). For the fixed RC scheme, the RC ratio is set to be 0.3, 0.5 and 0.7, respectively. For the random RC scheme, the RC ratio follows a uniform distribution over the closed interval $[0, 1]$. It can be observed that as the circuit power consumption increases, the outage capacity decreases. This is because with the increasing of the circuit power consumption, the outage probability will increase due to the fact that most of received signals will be harvested to power the circuit operation, resulting in a smaller received SINR at the BR. Besides, a larger outage probability leads to a smaller outage capacity. By comparisons, we can see that the proposed scheme can achieve the best performance since the proposed scheme provides more flexibility to utilize the resource efficiently.

B. The impact of backscatter links on the legacy transmission

Fig. 4 plots the outage probability for the legacy transmission as a function of the transmit power of the LT, where four cases are considered. The first case is the case without
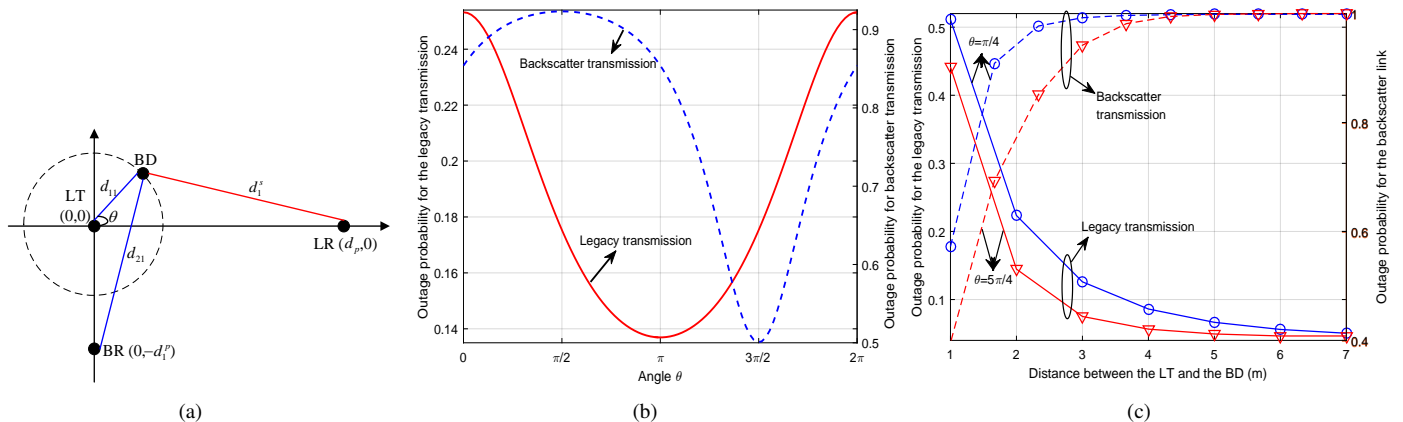
Fig. 6. (a) Relative locations among the LT, LR, BD and BR. (b) The impact of the location of the BD on outage probabilities for the legacy and backscatter transmissions. (c) Outage probabilities for the legacy and backscatter transmissions versus the distance between the LT and the BD.

backscatter transmission. In this case, the legacy transmission will not be interfered and the outage probability for the legacy transmission is given by (29). The second case is the case where the k-th ($k \in \{1, 2, 3\}$) BD is selected and the outage probability of the legacy transmission is determined by (23). The third case is the best case where the backscatter link with the minimum interference on the legacy link is selected for backscattering and the outage probability of this case is given by (28). The fourth case is the worst case where the backscatter link with the maximum interference on the legacy link is selected and the outage probability is computed based on (38). One observation is that there is an exact agreement between the derived results and the Monte Carlo simulation results. Besides, we also observe that the outage probability of the legacy transmission with an interference from the backscatter link is generally inferior to that of the legacy transmission with no interference. Due to the existence of the interference, there exists an error floor for the outage probability of the legacy transmission. Another observation is that the outage probability under the best case is lowest among the cases with interferences while the outage probability under the worst case is highest. In addition, the selected backscatter link with the minimum interference for backscattering is helpful to reduce error floor and eliminate the bad influence as much as possible. Also, we can find that the results with the linear model can not catch the outage performance of the real systems, but the gap caused by the inaccurate energy harvesting mode is smaller than the backscatter system.

Fig. 5 shows the outage probability of the legacy transmission versus the given transmission rate R_{th}, where P_t is set as 30 dBm. It can be observed that with the increasing of R_{th}, all the outage probabilities firstly increase and then equal one. For example, when R_{th} is large enough, i.e., $R_{\text{th}} \geq 18$ Mbps, all the outage probabilities are always one. This observation is refer to as rate ceiling. In addition, it can also be found that the outage probability of the best case is lowest and the corresponding rate ceiling is the largest.

C. Trade-off for the outage performance between the legacy transmission and the backscatter link

In order to study the impact of the location of the BD on the both legacy and backscatter links, we consider a specific scenario which consists of one LT, one LR, one BD and one BR, as shown in Fig. 6(a). In particular, the LT is located at the origin $(0, 0)$. The LR and the BR lie on the x-axis with $(d_p, 0)$ and the y-axis with $(0, -d_1^p)$, respectively. Assume that the BD moves on a circle of radius d_{11} centered around the origin. Denote the angle between the radius and the x-axis as θ. Then d_{21} and d_1^s are computed as $d_{21} = \sqrt{d_{11}^2 + (d_1^p)^2 - 2d_{11}d_1^p \cos\left(\theta + \frac{\pi}{2}\right)}$ and $d_1^s = \sqrt{d_{11}^2 + (d_p)^2 - 2d_{11}d_p \cos(\theta)}$, respectively. Let d_p, d_{11} and d_1^p be 10 m, 2 m and 4 m.

Fig. 6(b) plots the outage probabilities of the legacy transmission and the backscatter link versus θ for the considered scenario. It can be observed that the outage probability of the legacy link decreases when the angle varies in the range of $[0, \pi]$ and increases within $[\pi, 2\pi]$, while the outage probability of the backscatter transmission increases within the ranges of $[0, \frac{\pi}{2}]$ and $[\frac{3\pi}{2}, 2\pi]$ and decreases within $[\frac{\pi}{2}, \frac{3\pi}{2}]$. It can be found that the minimum outage probabilities for the legacy and the backscatter transmissions are achieved at $\theta = \pi$ and $\theta = \frac{3\pi}{2}$, respectively. With $\theta \in [0, \frac{\pi}{2}]$ (or $\theta \in [\pi, \frac{3\pi}{2}]$), a better outage performance for the legacy (or backscatter) link is achieved at the cost of the backscatter (legacy) transmission's performance. With $\theta \in [\frac{\pi}{2}, \pi]$, a win-win situation will be achieved and when $\theta \in [\frac{3\pi}{2}, 2\pi]$, the outage performance of both the legacy and the backscatter links will become worse, which needs to be avoided. It is worth noting that the win-win area can be enlarged by adjusting the location of the BR with d_1^p unchanged. For example, when the BR in Fig. 6(a) moves away from the LR in a clockwise direction with d_1^p unchanged, the bule dotted line in Fig. 6(b) will move the same angle to the left and the win-win area also increases. When the BR is located at $(-d_1^p, 0)$ (the opposite direction of the LR), the win-win area is $\theta \in [0, \pi]$, which is the largest. When the BR is located at $(d_1^p, 0)$, there is no win-win area in this case. Besides, we can also get some insights for the

deployment of the BD. For example, we can choose a proper angle to minimize the outage probability of the backscatter link while satisfying a given outage constraint for the legacy transmission.

Fig. 6(c) shows the impact of d_{11} on the outage probabilities of the legacy transmission and the backscatter link, where θ is fixed as $\frac{\pi}{4}$ and $\frac{5\pi}{4}$, respectively. It can be observed that with the increasing of d_{11}, the outage probabilities of the legacy transmission decrease while the outage probabilities of the backscatter link increase. This is because the received RF power decreases with the increasing of d_{11}, resulting in a smaller backscattered signal at both the LR and the BR. It can also be found that under the given outage constraint for the legacy link, it is better to choose a smaller d_{11} to achieve a better outage performance of the backscatter transmission.

VI. Conclusions

In this work, we have studied the outage performance for AmBackComs. Specifically, we have proposed an adaptive RC to minimize the outage probability for any given backscatter link. With a given backscatter link and the optimal RC ratio, we derived the outage probabilities for the backscatter system and the legacy transmission, respectively. Besides, the best and worst outage performances of the backscatter system and the legacy transmission have been investigated, respectively. Simulation results have verified the correctness of our analytical results and provided practical insights into the impacts of the co-channel interference, the EH model, and the location of BDs. Key observations have been summarized as follows. Firstly, the co-channel interference leads to the outage saturation phenomenon in the backscatter and legacy links. Besides, the backscatter transmission leads to a rate ceiling for the legacy link. Secondly, selecting the backscatter link with the lowest interference on the LR ensures that the performance loss of the legacy link is kept to a minimum. Thirdly, the conventionally used linear EH model will result in an over-estimated outage performance for the backscatter link while the impact on the legacy link is very small.

Appendix A

We first compute $\mathbb{P}(S_k \leq x, |h_{1k}|^2 \geq \frac{b_k}{a_k})$ as

$$
\begin{aligned}
&\mathbb{P}(S_k \leq x, |h_{1k}|^2 \geq \frac{b_k}{a_k}) \\
&\overset{(a)}{=} \int_{\frac{b_k}{a_k}}^{+\infty} \left[1 - \exp\left(-\frac{x}{\lambda_{2k}(a_k y - b_k)} \right) \right] \frac{e^{-\frac{y}{\lambda_{1k}}}}{\lambda_{1k}} dy \\
&\overset{(b)}{=} \left(1 - \frac{1}{\lambda_{1k} a_k} \int_0^{+\infty} \exp\left(-\frac{x}{\lambda_{2k} z} - \frac{z}{a_k \lambda_{1k}} \right) dz \right) \\
&\quad \times \exp\left(-\frac{b_k}{a_k \lambda_{1k}} \right),
\end{aligned} \tag{A.1}
$$

where steps (a) and (b) follows from $y = |h_{1k}|^2$ and $z = a_k y - b_k$, respectively. Then $F_{S_k}(x)$ can be calculated as

$$
\begin{aligned}
F_{S_k}(x) &= \mathbb{P}(S_k \leq x \big| |h_{1k}|^2 \geq \frac{b_k}{a_k}) \\
&= \frac{\mathbb{P}(S_k \leq x, |h_{1k}|^2 \geq \frac{b_k}{a_k})}{\mathbb{P}(|h_{1k}|^2 \geq \frac{b_k}{a_k})} \\
&= 1 - \frac{1}{\lambda_{1k} a_k} \int_0^{+\infty} \exp\left(-\frac{x}{\lambda_{2k} z} - \frac{z}{a_k \lambda_{1k}} \right) dz \\
&\overset{(c)}{=} 1 - \frac{1}{\lambda_{1k} a_k} \sqrt{\frac{4 a_k \lambda_{1k} x}{\lambda_{2k}}} K_1\left(\sqrt{\frac{4x}{\lambda_{2k} \lambda_{1k} a_k}} \right), \quad \text{(A.2)}
\end{aligned}
$$

where step (c) holds based on [3.324] in [36] and $K_1(\cdot)$ is the modified Bessel function of the second kind.

Further, the PDF of S_k conditioned on $|h_{1k}|^2 \geq \frac{b_k}{a_k}$ is

$$
\begin{aligned}
f_{S_k}(x) &= \frac{\partial \mathbb{P}(S_k \leq x \big| |h_{1k}|^2 \geq \frac{b_k}{a_k})}{\partial x} \\
&= \frac{1}{\lambda_{1k} \lambda_{2k} a_k} \int_0^{+\infty} \frac{1}{z} \exp\left(-\frac{x}{\lambda_{2k} z} - \frac{z}{a_k \lambda_{1k}} \right) dz \\
&\overset{(d)}{=} \frac{2}{\lambda_{1k} \lambda_{2k} a_k} K_0\left(2\sqrt{\frac{x}{\lambda_{1k} \lambda_{2k} a_k}} \right), \quad \text{(A.3)}
\end{aligned}
$$

where step (d) follows by [3.478] in [36] and $K_0(\cdot)$ is the modified Bessel function of the second kind.

Appendix B

Following $|h_{1k}|^2 \sim \exp(\frac{1}{\lambda_{1k}})$, we can compute I_1 as

$$
I_1 = 1 - \exp\left(-\frac{b_k}{a_k \lambda_{1k}} \right). \tag{B.1}
$$

Then the main difficulty is how to compute I_2. In order to obtain I_2, we first provide the following proposition to achieve both the CDF and PDF with respect to S_k conditioned on $|h_{1k}|^2 \geq \frac{b_k}{a_k}$.

By means of Proposition 1, we can calculate I_2 as

$$
\begin{aligned}
I_2 &= \mathbb{P}\left(\frac{S_k}{P_t K_k^p |g_k^p|^2 + \sigma^2} < \gamma_{\text{th}}^b \bigg| |h_{1k}|^2 \geq \frac{b_k}{a_k} \right) \\
&\quad \times \mathbb{P}\left(|h_{1k}|^2 \geq \frac{b_k}{a_k} \right) \\
&\overset{(a)}{=} (1 - I_1) \Bigg[\underbrace{\int_{\gamma_{\text{th}}^b \sigma^2}^{+\infty} \exp\left(-\frac{x}{\gamma_{\text{th}}^b P_t K_k^p \lambda_k^p} \right) f_{S_k}(x) \, dx}_{I_{2-1}} \\
&\quad \times \exp\left(\frac{\sigma^2}{P_t K_k^p \lambda_k^p} \right) + F_{S_k}\left(\gamma_{\text{th}}^b \sigma^2 \right) \Bigg], \quad \text{(B.2)}
\end{aligned}
$$

where step (a) follows by letting $|g_k^p|^2 \sim \exp(\frac{1}{\lambda_k^p})$ and considering two cases, i.e., $S_k > \gamma_{\text{th}}^b \sigma^2$ and $S_k \leq \gamma_{\text{th}}^b \sigma^2$.

Further, I_{2-1} can be rewritten as

$$
\begin{aligned}
I_{2-1} &= I_{2-2} - \int_0^{\gamma_{\text{th}}^b \sigma^2} \exp\left(-\frac{x}{\gamma_{\text{th}}^b P_t K_k^p \lambda_k^p} \right) f_{S_k}(x) \, dx \\
&\overset{(b)}{=} \Theta_k - \int_0^{\gamma_{\text{th}}^b \sigma^2} \exp\left(-\frac{x}{\gamma_{\text{th}}^b P_t K_k^p \lambda_k^p} \right) f_{S_k}(x) \, dx,
\end{aligned} \tag{B.3}
$$

where $I_{2-2} = \int_0^{+\infty} \exp\left(-\frac{x}{\gamma_{\text{th}}^b P_t K_k^p \lambda_k^p}\right) f_{S_k}(x)\,dx$, step (b) follows from Appendix C and $\Theta_k = -\vartheta_k \gamma_{\text{th}}^b \text{Ei}(-\vartheta_k \gamma_{\text{th}}^b)\exp\left(\vartheta_k \gamma_{\text{th}}^b\right)$ with $\vartheta_k = \frac{P_t K_k^p \lambda_k^p}{\lambda_{1k}\lambda_{2k}a_k}$ and the exponential integral function $\text{Ei}(\varrho) = \int_{-\infty}^{\varrho} t^{-1}e^t dt$.

APPENDIX C

Let α_1 and α_2 denote $\frac{1}{\gamma_{\text{th}}^b P_t K_k^p \lambda_k^p}$ and $\frac{1}{\lambda_{1k}\lambda_{2k}a_k}$, respectively. Then I_{2-2} can be calculated as

$$
\begin{aligned}
I_{2-2} &= \frac{2}{\lambda_{1k}\lambda_{2k}a_k}\int_0^{+\infty} e^{-\alpha_1 x}K_0\left(2\sqrt{\alpha_2 x}\right)dx \\
&\overset{(a)}{=} \frac{e^{\frac{\alpha_2}{2\alpha_1}}}{\lambda_{1k}\lambda_{2k}a_k\sqrt{\alpha_1\alpha_2}}(\Gamma(1))^2 W_{-\frac{1}{2},0}\left(\frac{\alpha_2}{\alpha_1}\right) \\
&= \frac{1}{\lambda_{1k}\lambda_{2k}a_k\alpha_1}\int_0^{+\infty}\frac{e^{-\frac{\alpha_2 t}{\alpha_1}}}{1+t}dt \\
&= \frac{-e^{\frac{\alpha_2}{\alpha_1}}}{\lambda_{1k}\lambda_{2k}a_k\alpha_1}\text{Ei}\left(-\frac{\alpha_2}{\alpha_1}\right) \\
&\overset{(b)}{=} -\vartheta_k\gamma_{\text{th}}^b\text{Ei}(-\vartheta_k\gamma_{\text{th}}^b)\exp\left(\vartheta_k\gamma_{\text{th}}^b\right),
\end{aligned}
\tag{C.1}
$$

where step (a) holds based on [6.614] in [36]; $\Gamma(x) = \int_0^{+\infty}t^{x-1}e^{-t}dt$ is a gamma function; $W_{\mu,\nu}(x)$ is a Whittaker function which is given by $W_{\mu,\nu}(x) = \frac{x^{\nu+0.5}e^{-\frac{x}{2}}}{\Gamma(\nu-\mu+0.5)}\int_0^{+\infty}e^{-xt}t^{\nu-\mu-0.5}(1+t)^{\nu+\mu-0.5}dt$; $\text{Ei}(\varrho) = \int_{-\infty}^{\varrho}t^{-1}e^t dt$ denotes the exponential integral function; step (b) follows by letting $\vartheta_k = \frac{P_t K_k^p \lambda_k^p}{\lambda_{1k}\lambda_{2k}a_k}$.

APPENDIX D

In (14), the term $\int_0^{\gamma_{\text{th}}^b\sigma^2}\exp\left(-\frac{x}{\gamma_{\text{th}}^b P_t K_k^p \lambda_k^p}\right)f_{S_k}(x)\,dx$ is not a closed-form expression. Thus the purpose of this appendix to approximate this term based on a high transmit power of the LT.

$$
\begin{aligned}
&\int_0^{\gamma_{\text{th}}^b\sigma^2}\exp\left(-\frac{x}{\gamma_{\text{th}}^b P_t K_k^p \lambda_k^p}\right)f_{S_k}(x)\,dx \\
&\overset{(a)}{=} \frac{-2}{\lambda_{1k}\lambda_{2k}a_k}\int_0^{\gamma_{\text{th}}^b\sigma^2}\exp\left(-\frac{x}{\gamma_{\text{th}}^b P_t K_k^p \lambda_k^p}\right)\ln\left(\sqrt{\frac{x}{\lambda_{1k}\lambda_{2k}a_k}}\right)dx \\
&\quad -\frac{2}{\lambda_{1k}\lambda_{2k}a_k}\int_0^{\gamma_{\text{th}}^b\sigma^2}c_0\exp\left(-\frac{x}{\gamma_{\text{th}}^b P_t K_k^p \lambda_k^p}\right)dx \\
&\overset{(b)}{=} \frac{-4}{\lambda_{1k}\lambda_{2k}a_k}\int_0^{\sqrt{\gamma_{\text{th}}^b}\sigma}y\exp\left(-\frac{y^2}{\gamma_{\text{th}}^b P_t K_k^p \lambda_k^p}\right)\ln\left(\frac{y}{\sqrt{\lambda_{1k}\lambda_{2k}a_k}}\right)dy \\
&\quad -2\gamma_{\text{th}}^b\vartheta_k c_0\left(1-\exp\left(-\frac{\sigma^2}{P_t K_k^p \lambda_k^p}\right)\right).
\end{aligned}
\tag{D.1}
$$

where step (a) holds from $K_0(x) \approx -\ln\left(\frac{x}{2}\right) - c_0$ at $x \to 0$ [eq. (8.446), [36]] and the fact that the noise power is very small in practical communications, i.e., $\sigma^2 \to 0$; $c_0 \approx 0.5772$ is the Euler constant; step (b) is derived from the variable substitution, i.e., $y = \sqrt{x}$.

Based on the fourier series of $\exp\left(-\frac{x^2}{\gamma_{\text{th}}^b P_t K_k^p \lambda_k^p}\right)$ at $x \to 0$ [eq.(1.211.3), [36]], we have the following approximation when the transmit power of the LT is high, given by

$$
\begin{aligned}
&\int_0^{\sqrt{\gamma_{\text{th}}^b}\sigma}y\exp\left(-\frac{y^2}{\gamma_{\text{th}}^b P_t K_k^p \lambda_k^p}\right)\ln\left(\frac{y}{\sqrt{\lambda_{1k}\lambda_{2k}a_k}}\right)dy \\
&\approx \int_0^{\sqrt{\gamma_{\text{th}}^b}\sigma}y\ln\left(\frac{y}{\sqrt{\lambda_{1k}\lambda_{2k}a_k}}\right)dy \\
&\quad -\int_0^{\sqrt{\gamma_{\text{th}}^b}\sigma}\frac{y^3}{\gamma_{\text{th}}^b P_t K_k^p \lambda_k^p}\ln\left(\frac{y}{\sqrt{\lambda_{1k}\lambda_{2k}a_k}}\right)dy \\
&= \frac{1}{2}\gamma_{\text{th}}^b\sigma^2\left(\ln\left(\frac{\sqrt{\gamma_{\text{th}}^b}\sigma}{\sqrt{\lambda_{1k}\lambda_{2k}a_k}}\right)-\frac{1}{2}\right) \\
&\quad -\frac{\gamma_{\text{th}}^b\sigma^4}{4P_t K_k^p \lambda_k^p}\left(\ln\left(\frac{\sqrt{\gamma_{\text{th}}^b}\sigma}{\sqrt{\lambda_{1k}\lambda_{2k}a_k}}\right)-\frac{1}{4}\right).
\end{aligned}
\tag{D.2}
$$

APPENDIX E

We first provide the CDF of G_k. Similar to (A.1), $\mathbb{P}\left(G_k \le x, |h_{1k}|^2 > \frac{b_k}{a_k}\right)$ is given by

$$
\begin{aligned}
&\mathbb{P}\left(G_k \le x, |h_{1k}|^2 > \frac{b_k}{a_k}\right) \\
&= \left(1-\frac{1}{\lambda_{1k}a_{ik}}\sqrt{\frac{4a_{ik}\lambda_{1k}x}{\lambda_k^s}}K_1\left(\sqrt{\frac{4x}{\lambda_{1k}\lambda_k^s a_{ik}}}\right)\right) \\
&\quad \times \exp\left(-\frac{b_k}{a_k\lambda_{1k}}\right).
\end{aligned}
\tag{E.1}
$$

Then the CDF of $\min(G_1, G_2, \ldots, G_K)$ conditioned on $\bigcap_{k=1}^K |h_{1k}|^2 > \frac{b_k}{a_k}$, denoted by $F_{G_{\min}}(x)$, is given by

$$
\begin{aligned}
&F_{G_{\min}}(x) \\
&= \mathbb{P}\left(\min(G_1, G_2, \ldots, G_K) \le x \,\middle|\, \bigcap_{k=1}^K |h_{1k}|^2 > \frac{b_k}{a_k}\right) \\
&= 1-\mathbb{P}\left(G_1 > x, G_2 > x, \ldots, G_K > x \,\middle|\, \bigcap_{k=1}^K |h_{1k}|^2 > \frac{b_k}{a_k}\right) \\
&= 1-\prod_{k=1}^K \frac{\mathbb{P}\left(G_k > x, |h_{1k}|^2 > \frac{b_k}{a_k}\right)\prod_{i=1,i\neq k}^K \mathbb{P}\left(|h_{1i}|^2 > \frac{b_i}{a_i}\right)}{\mathcal{P}_1} \\
&= 1-\prod_{k=1}^K\left[\frac{1}{\lambda_{1k}a_{ik}}\sqrt{\frac{4a_{ik}\lambda_{1k}x}{\lambda_k^s}}K_1\left(\sqrt{\frac{4x}{\lambda_{1k}\lambda_k^s a_{ik}}}\right)\right].
\end{aligned}
\tag{E.2}
$$

Appendix F

Based on the expression of $\widehat{G}_k$, we first determine the CDF of $\widehat{G}_k$ as

$$
\begin{aligned}
&\mathbb{P}\left(\widehat{G}_k \le x\right) \\
&= \mathbb{P}\left(G_k \le x, |h_{1k}|^2 > \frac{b_k}{a_k}\right) + \mathbb{P}\left(|h_{1k}|^2 \le \frac{b_k}{a_k}\right) \\
&= 1 - \frac{1}{\lambda_{1k}a_{ik}}\sqrt{\frac{4a_{ik}\lambda_{1k}x}{\lambda_k^s}}K_1\left(\sqrt{\frac{4x}{\lambda_{1k}\lambda_k^s a_{ik}}}\right) \\
&\times \exp\left(-\frac{b_k}{a_k\lambda_{1k}}\right).
\end{aligned}
\tag{F.1}
$$

Then the CDF of $\widehat{G}_{\max}$ can be calculated as

$$
\begin{aligned}
&F_{\widehat{G}_{\max}}(x) \\
&= \mathbb{P}\left(\max\left(\widehat{G}_1, \widehat{G}_2, \ldots, \widehat{G}_K\right) \le x\right) \\
&= \prod_{k=1}^{K}\left(1 - \frac{1}{\lambda_{1k}a_{ik}}\sqrt{\frac{4a_{ik}\lambda_{1k}x}{\lambda_k^s}}K_1\left(\sqrt{\frac{4x}{\lambda_{1k}\lambda_k^s a_{ik}}}\right)\right) \\
&\times \exp\left(-\frac{b_k}{a_k\lambda_{1k}}\right) + 1 - \exp\left(-\frac{b_k}{a_k\lambda_{1k}}\right).
\end{aligned}
\tag{F.2}
$$

References

[1] F. Jejdling, "Ericsson mobility report," https://www.ericsson.com/49d1d9/assets/local/mobility-report/documents/2019/ericsson-mobility-report-june-2019.pdf, Jun. 2019.

[2] N. V. Huynh, D. T. Hoang, X. Lu, D. Niyato, P. Wang, and D. I. Kim, "Ambient backscatter communications: A contemporary survey," *IEEE Commun. Surv. Tutor.*, vol. 20, no. 4, pp. 2889–2922, Fourthquarter 2018.

[3] 6G Flagship, "Key drivers and research challenges for 6G ubiquitous wireless intelligence (white paper)," http://jultika.oulu.fi/files/isbn9789526223544.pdf, Sep. 2019.

[4] J. Kimionis, A. Bletsas, and J. N. Sahalos, "Increased range bistatic scatter radio," *IEEE Trans. Commun.*, vol. 62, no. 3, pp. 1091–1104, Mar. 2014.

[5] Y. Ye, L. Shi, R. Q. Hu, and G. Lu, "Energy-efficient resource allocation for wirelessly powered backscatter communications," *IEEE Commun. Lett.*, vol. 23, no. 8, pp. 1418–1422, Aug. 2019.

[6] B. Kellogg *et al.*, "Wi-Fi backscatter: Internet connectivity for RF-powered devices," in *Proc. ACM SIGCOMM*, Aug. 2014, pp. 607–618.

[7] G. Wang, F. Gao, R. Fan, and C. Tellambura, "Ambient backscatter communication systems: Detection and performance analysis," *IEEE Trans. Commun.*, vol. 64, no. 11, pp. 4836–4846, Nov. 2016.

[8] J. Qian, F. Gao, G. Wang, S. Jin, and H. Zhu, "Semi-coherent detection and performance analysis for ambient backscatter system," *IEEE Trans. Commun.*, vol. 65, no. 12, pp. 5266–5279, Dec. 2017.

[9] Q. Tao, C. Zhong, X. Chen, H. Lin, and Z. Zhang, "Maximum-eigenvalue detector for multiple antenna ambient backscatter communication systems," *IEEE Trans. Veh. Technol.*, vol. 68, no. 12, pp. 12411–12415, Dec. 2019.

[10] G. Yang, Y. Liang, R. Zhang, and Y. Pei, "Modulation in the air: Backscatter communication over ambient OFDM carrier," *IEEE Trans. Commun.*, vol. 66, no. 3, pp. 1219–1233, Mar. 2018.

[11] D. T. Hoang, D. Niyato, P. Wang, D. I. Kim, and Z. Han, "Ambient backscatter: A new approach to improve network performance for RF-powered cognitive radio networks," *IEEE Trans. Commun.*, vol. 65, no. 9, pp. 3659–3674, Sep. 2017.

[12] X. Lu, D. Niyato, H. Jiang, D. I. Kim, Y. Xiao, and Z. Han, "Ambient backscatter assisted wireless powered communications," *IEEE Wireless Commun.*, vol. 25, no. 2, pp. 170–177, Apr. 2018.

[13] N. Van Huynh, D. T. Hoang, D. Niyato, P. Wang, and D. I. Kim, "Optimal time scheduling for wireless-powered backscatter communication networks," *IEEE Wireless Commun. Lett.*, vol. 7, no. 5, pp. 820–823, Oct. 2018.

[14] X. Gao, P. Wang, D. Niyato, K. Yang, and J. An, "Auction-based time scheduling for backscatter-aided RF-powered cognitive radio networks," *IEEE Trans. Wireless Commun.*, vol. 18, no. 3, pp. 1684–1697, Mar. 2019.

[15] S. H. Kim and D. I. Kim, "Hybrid backscatter communication for wireless-powered heterogeneous networks," *IEEE Trans. Wireless Commun.*, vol. 16, no. 10, pp. 6557–6570, Oct. 2017.

[16] B. Lyu, H. Guo, Z. Yang, and G. Gui, "Throughput maximization for hybrid backscatter assisted cognitive wireless powered radio networks," *IEEE Internet Things J.*, vol. 5, no. 3, pp. 2015–2024, Jun. 2018.

[17] D. T. Hoang, D. Niyato, P. Wang, and D. I. Kim, "Optimal time sharing in RF-powered backscatter cognitive radio networks," in *Proc. IEEE ICC*, May 2017, pp. 1–6.

[18] X. Gao, D. Niyato, P. Wang, K. Yang, and J. An, "Contract design for time resource assignment and pricing in backscatter-assisted RF-powered networks," *IEEE Wireless Commun. Lett.*, vol. 9, no. 1, pp. 42–46, Jan. 2020.

[19] X. Kang, Y. Liang, and J. Yang, "Riding on the primary: A new spectrum sharing paradigm for wireless-powered IoT devices," *IEEE Trans. Wireless Commun.*, vol. 17, no. 9, pp. 6335–6347, Sep. 2018.

[20] G. Yang, D. Yuan, Y. Liang, R. Zhang, and V. C. M. Leung, "Optimal resource allocation in full-duplex ambient backscatter communication networks for wireless-powered IoT," *IEEE Internet Things J.*, vol. 6, no. 2, pp. 2612–2625, Apr. 2019.

[21] W. Zhao, G. Wang, R. Fan, L. Fan, and S. Atapattu, "Ambient backscatter communication systems: Capacity and outage performance analysis," *IEEE Access*, vol. 6, no. 1, pp. 22695–22704, Apr. 2018.

[22] D. Darsena, G. Gelli, and F. Verde, "Modeling and performance analysis of wireless networks with ambient backscatter devices," *IEEE Trans. Commun.*, vol. 65, no. 4, pp. 1797–1814, Apr. 2017.

[23] S. Zhou, W. Xu, K. Wang, C. Pan, M. Alouini, and A. Nallanathan, "Ergodic rate analysis of cooperative ambient backscatter communication," *IEEE Wireless Commun. Lett.*, vol. 8, no. 6, pp. 1679–1682, Dec. 2019.

[24] D. Li, "Two birds with one stone: Exploiting decode-and-forward relaying for opportunistic ambient backscattering," *IEEE Trans. Commun.*, doi. 10.1109/TCOMM.2019.2957490 2019.

[25] D. Li and Y. Liang, "Adaptive ambient backscatter communication systems with MRC," *IEEE Trans. Veh. Technol.*, vol. 67, no. 12, pp. 12352–12357, Dec. 2018.

[26] L. Xu, K. Zhu, R. Wang, and S. Gong, "Performance analysis of ambient backscatter communications in RF-powered cognitive radio networks," in *Proc. IEEE WCNC*, Apr. 2018, pp. 1–6.

[27] W. Zhao, G. Wang, S. Atapattu, C. Tellambura, and H. Guan, "Outage analysis of ambient backscatter communication systems," *IEEE Commun. Lett.*, vol. 22, no. 8, pp. 1736–1739, Aug. 2018.

[28] S. T. Shah, K. W. Choi, T. Lee, and M. Y. Chung, "Outage probability and throughput analysis of SWIPT enabled cognitive relay network with ambient backscatter," *IEEE Internet Things J.*, vol. 5, no. 4, pp. 3198–3208, Aug. 2018.

[29] X. Lu, H. Jiang, D. Niyato, D. I. Kim, and Z. Han, "Wireless-powered device-to-device communications with ambient backscattering: Performance modeling and analysis," *IEEE Trans. Wireless Commun.*, vol. 17, no. 3, pp. 1528–1544, Mar. 2018.

[30] S. Wang, M. Xia, K. Huang, and Y. Wu, "Wirelessly powered two-way communication with nonlinear energy harvesting model: Rate regions under fixed and mobile relay," *IEEE Trans. Wireless Commun.*, vol. 16, no. 12, pp. 8190–8204, Dec. 2017.

[31] Y. Liu, Y. Ye, H. Ding, F. Gao, and H. Yang, "Outage performance analysis for SWIPT-based incremental cooperative NOMA networks with non-linear harvester," *IEEE Commun. Lett.*, vol. 24, no. 2, pp. 287–291, Feb 2020.

[32] T. Le, K. Mayaram, and T. Fiez, "Efficient far-field radio frequency energy harvesting for passively powered sensor networks," *IEEE J. Solid State Circuits*, vol. 43, no. 5, pp. 1287–1302, May 2008.

[33] S. Ma, G. Wang, R. Fan, and C. Tellambura, "Blind channel estimation for ambient backscatter communication systems," *IEEE Commun. Lett.*, vol. 22, no. 6, pp. 1296–1299, Jun. 2018.

[34] L. Shi, Y. Ye, R. Q. Hu, and H. Zhang, "System outage performance for three-step two-way energy harvesting DF relaying," *IEEE Trans. Veh. Technol.*, vol. 68, no. 4, pp. 3600–3612, Apr. 2019.

[35] L. Zheng and D. N. C. Tse, "Diversity and multiplexing: a fundamental tradeoff in multiple-antenna channels," *IEEE Trans. Inform. Theory*, vol. 49, no. 5, pp. 1073–1096, May 2003.

[36] I. S. Gradshteyn and I. M. Ryzhik, *Table of integrals, series, and products*, 7th ed. New York, NY, USA: Academic press, 2007.

[37] Y. Ye, L. Shi, X. Chu, H. Zhang, and G. Lu, "On the outage performance of SWIPT-based three-step two-way DF relay networks," *IEEE Trans. Veh. Technol.*, vol. 68, no. 3, pp. 3016–3021, Mar. 2019.

[38] Y. Liu, Z. Ding, M. Elkashlan, and H. V. Poor, "Cooperative non-orthogonal multiple access with simultaneous wireless information and power transfer," *IEEE J. Sel. Areas Commun.*, vol. 34, no. 4, pp. 938–953, Apr. 2016.